ACS Combinatorial Science

Technology Note

pubs.acs.org/acscombsci

High-Throughput Analysis of Molecular Orientation on Surfaces by NEXAFS Imaging of Curved Sample Arrays

Joe E. Baio,[†,§] Cherno Jaye,[‡] Daniel A. Fischer,[‡,*] and Tobias Weidner*[,†]

[†]Max Planck Institute for Polymer Research, 55128 Mainz, Germany

[‡]National Institute of Standards and Technology, Gaithersburg, Maryland 20899, United States

ABSTRACT: Near-edge X-ray absorption fine structure (NEXAFS) spectroscopy provides detailed information about the orientation and alignment of thin films. NEXAFS is a synchrotron-based technique—the availability of beam-time per user is typically limited to no more than a few weeks per year. The limited availability is currently a true barrier for using NEXAFS in combinatorial studies of molecular alignment. We have recently demonstrated how large area full field NEXAFS imaging allows users to pursue combinatorial studies of surface chemistry. Now we report an extension of this approach which allows the acquisition of orientation information from a single NEXAFS image. An array with 80 elements (samples), containing eight series of different surface modifications, was mounted on a curved substrate allowing the collection of NEXAFS spectra with a range of orientations with respect to the X-ray beam. Images collected from this array show how hyperspectral NEXAFS data collected from curved surfaces can be used for high-throughput molecular orientation analysis.

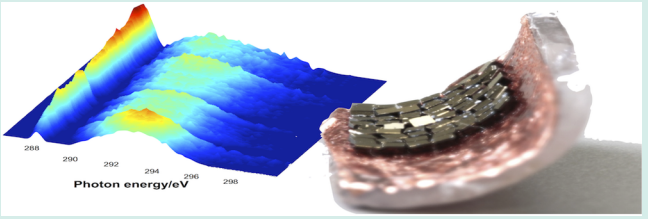

KEYWORDS: *self-assembled monolayers, combinatorial science, imaging NEXAFS, alkanethiol, angle-resolved photoemission, molecular order*

Rational, structure-based design is the most elegant and direct method for developing new materials. Many functional materials are structurally complex, and the precise correlation of the preparative approach, material structure, and ultimately performance is often not well understood. Time consuming synthesis and costly screening of candidate materials could be avoided by a thorough understanding of the underlying chemistry driving material properties. As a result, the development of new materials can be accelerated by combinatorial material screening methods, evaluating massive numbers of samples, to identify promising "lead" materials and synthesis methods.[1] Combinatorial approaches have the potential to enable the conception and preparation of new surfaces with surprising properties, especially for catalytic, electronic, and medical applications.[1] Self-assembled monolayers (SAMs) are very promising in this context.[2] For applications where the orientation and structural alignment are crucial for device performance SAMs have been used to improve the performance of electronic devices,[3−9] while protein and DNA SAMs have been adopted as effective sensors in biochips.[10,11] For a SAM-based insulators, perfect order and tight packing of the molecular monolayer is crucial to avoid dielectric breakdown in a device.[12,13] In contrast, for top-contact organic field effect transistors, it has been shown, that an amorphous, liquid-like SAM structure is beneficial for charge carrier density and device performance.[7] In biochips, well-aligned protein films with active centers pointing toward the sensor medium are crucial for effective sensing.[11]

These examples illustrate that different applications have very specific requirements in terms of the structure and order of the SAMs used. The structure, order, and orientation of self-assembled films will depend on a large number of factors: the structure and architecture of target molecules and surfaces but also on many preparative parameters, such as temperature, pH, concentration, rinsing, adsorption time, and the solvent.

A method that can directly monitor molecular ordering and alignment at surfaces is near-edge X-ray absorption fine structure (NEXAFS) spectroscopy. This technique probes chemical bonds at surfaces by exciting core electrons into unoccupied molecular orbitals.[14] In addition, NEXAFS spectra contain valuable information about the orientation of surface species. NEXAFS measures the dependence of the photo-excitation cross section on the orientation of the electric field vector of the linearly polarized synchrotron light with respect to the transition dipole moment of the probed molecular orbital.[14,15] This effect is called linear dichroism in X-ray absorption. To determine the order and orientation of surface species, the photoemission of the absorption resonances changes in intensity as the incident angle of the synchrotron light is varied from glancing to normal angles with respect to the incoming X-ray beam. As the incident angle is varied relative changes in absorption intensities are monitored. This method has been used to track the structure of SAMs,[16−18] surfactants,[15] polymers,[19] and proteins[20−24] on surfaces.

Received: November 19, 2013
Published: July 21, 2014

NEXAFS spectroscopy requires access to a synchrotron user facility where instrument time is usually limited to no more than a few weeks per year. During a NEXAFS experiment it is typically only possible to analyze ∼20 samples per day; as a result, pursuing large-scale combinatorial studies with ≫100 samples would require prohibitively extended beam access. We have recently demonstrated, that by using a newly developed large area full field NEXAFS microscope at the National Institute of Standard and Technology (NIST) U7A beamline, at the National Synchrotron Light Source (NSLS), the sample throughput can be increased by a factor of 200. Thereby, opening up the possibility of applying NEXAFS to combinatorial studies. The microscope uses a magnetic lens to guide emitted photoelectrons onto a detector that provides a two-dimensional image of a 13 × 18 mm^2 sample region.[25] The lens is a gradient field where electrons emitted from the sample follow a set of expanding field lines to the detector. This gradient produces a 2× magnification which results in a large depth of field, thereby, allowing the direct imaging of a curved substrate. An advantage of this microscope over other photoelectron microscopic techniques using electric lenses is its ability to handle insulators and highly curved nonplanar surfaces.[26] The large full field imaging allows the parallel analysis of large arrays of samples arranged on a sample holder. We have recently demonstrated that such a multiplexed orientational and structural analysis by imaging NEXAFS (MOSAIX) approach enables the characterization of large sample sets required for combinatorial studies.[27] For orientational analysis, however, MOSAIX images at different X-ray incidence angle have to be acquired and the spectroscopic information extracted and analyzed. We here demonstrate that by using curved MOSAIX sample holders one can obtain orientation information from large sample sets in a single image without the need for acquisitions at multiple angles. Again, accelerating the high throughput screening of molecular orientation.

To demonstrate the high throughput determination of molecular orientation a model system based on a series of alkanethiol SAMs was prepared and analyzed with the NEXAFS microscope. The sample set consisted of an array of 1 × 1 mm^2 gold-coated silicon substrates arranged onto a 10 × 8 mm^2 curved sample holder. The sample holder curvature was equivalent to an arc of 90° (Figure 1). The gold surfaces were coated with alkanethiols at four different alkane chain lengths, ranging from 8 to 18 carbon atoms per chain (C8S, C10S, C12S, and C18S, see Scheme 1). The SAMs were prepared from 1 mM solutions of the respective compounds in ethanol and allowed to assemble for 16 h using previously described methods.[27,28] Two rows of duplicate samples per chain lengths were mounted. As shown in Figure 1, the rows of samples mounted on the curved holder leads to X-ray incidence angles at the samples ranging from 20° to 90°.

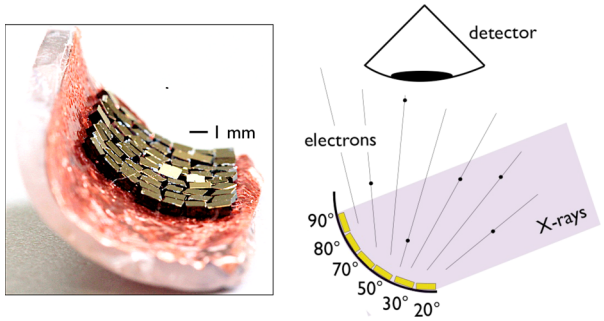

Figure 1. (a) Photo of the curved sample holder and the sample map. (b) Illustration of the sample arrangement and the experimental geometry.

Scheme 1. Drawing of the SAM Samples Prepared As Model Systems for the Curved Arrays[a]

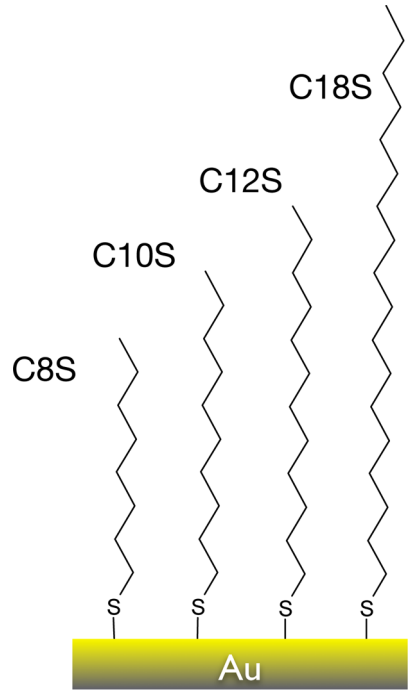

[a]Alkanethiols with varying chain length were assembled onto gold surfaces. Longer chain SAMs are expected to show a higher degree of orientational order.

Stacks of electron yield images of the array were collected at the carbon *K*-edge by stepping through the 270−360 eV photon energy range with a step size of 0.1 eV. Each pixel (stack) in the resulting image contained a full NEXAFS spectrum, allowing a detailed spectral analysis. Plotting images based on specific energy ranges allows the user to highlight specific molecular features of the SAMs. A NEXAFS spectrum recorded for C18S at an X-ray incidence angle of 20° was extracted from the array and is shown in Figure 2a. Mapping the intensities related to different spectral regions, as we scan the photon energy across the carbon the spectrum, we observe features corresponding to the Rydberg resonance (R^*) region near 287.5 eV related to C−H groups and at higher photon energies, σ^* C−C bonds. A very weak peak at ∼285.2 eV is also observed. This peak is explained either by an excitation into alkane-substrate orbitals,[29] or a normalization issue caused by carbon contamination on the beamline optics. Since radiation damage from the X-rays can also cause peaks to appear in this spectral range,[30] a careful beam damage study was performed to rule out this possibility.

Figure 2b displays a NEXAFS image of the array based on the total carbon electron yield near the carbon *K*-edge (285−312 eV). The image demonstrates that, when moving from longer to shorter SAM chain lengths (down in the array image), the intensity of the photoemission decreases. This is explained by the lower carbon content of the short chain compared to long chain SAMs.[31]

dx.doi.org/10.1021/co5001162 | ACS Comb. Sci. 2014, 16, 449−453

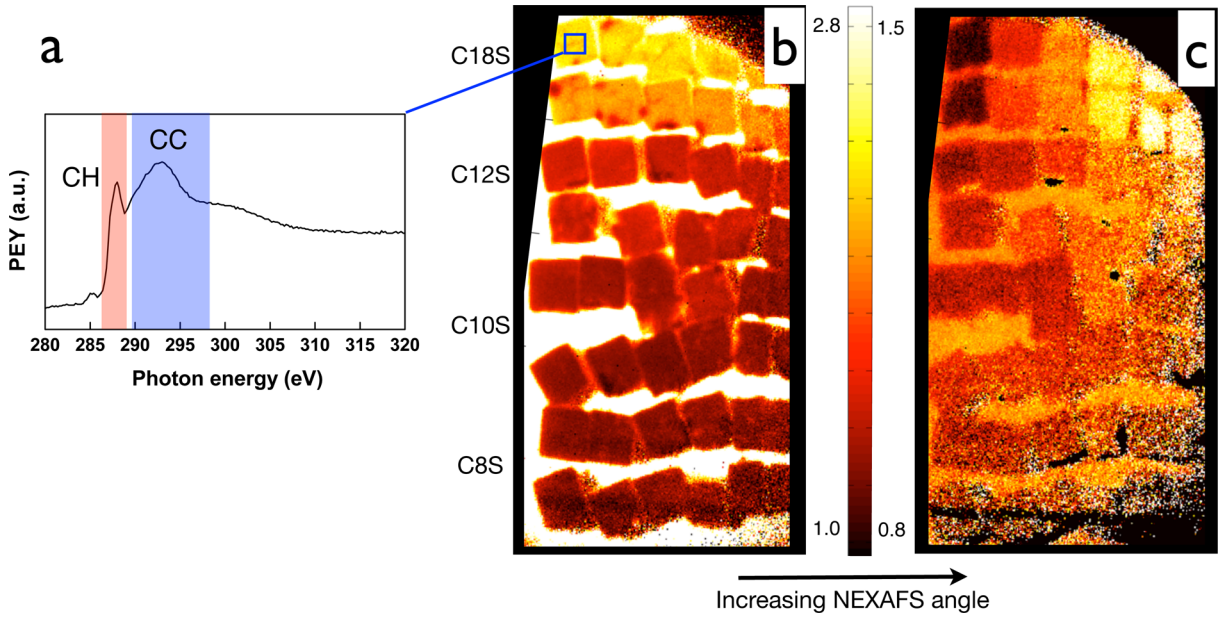

Figure 2. (a) NEXAFS spectrum for the C18S SAMs extracted from the array. σ^* CH and σ^* CC resonances are indicated. (b) Pre-edge normalized NEXAFS image of the curved MOSAIX array. The image contrast represents the total carbon content. (c) Intensity ratio image of the σ^* CH and the σ^* CC spectral region. Variations for increasing NEXAFS angles are indicative of molecular alignment. The C18S SAMs show the greatest alignment.

Orientation information about sample arrays can be obtained directly by dividing images of spectral features with opposite response to angle variations, such as the C−H and the C−C resonances in the alkanthiol SAM array. The sign of C−H and the C−C angle dependence is inverted because of the orthogonal orientation of the respective final state orbitals. An image based on the intensity in the C−H range (285.9−289.2 eV) divided by the intensity in the C−C range (289.4−297.4 eV) is shown in Figure 2c. The intensity changes, in this image, are directly related to the degree of order in the SAMs and gives a qualitative overview of molecular alignment over the large sample set. Along the direction of the substrate curvature (right in the array image) we see the C−H/C−C intensity ratio increases as we go to higher incidence angles. The angle dependence is more pronounced for the longer chain SAMs (C18S and C12S). A greater order observed for the long chain SAMs is in agreement with previous low-energy electron diffraction, reflection−absorption infrared spectroscopy[32] and NEXAFS[33,34] studies.

Two-dimensional plots of the electron yield, as a function of photon energy and position along the substrate curvature, can be used to analyze the linear dichroism in individual sample sets in more detail. Such 2D plots for the C10S and the C18S SAM are shown in Figure 3. The differences in the angle dependence, that is, orientational alignment, are directly visible. Having order information in a single image is an advantage over extracting order information from flat arrays at different angles. The involved processing and overlaying of images at different angles can be challenging because acquisition at different angles leads to image distortion. The limited fidelity of image correction limits the lateral resolution of surface order analysis.

A more quantitative analysis of the molecular orientation, in terms of tilt angles in an array, can be performed by first extracting spectra from pre- and postedge normalized images for samples along the curvature and then analyzing the angle dependence of the partial electron yield by well established methods.[14] Figure 4 shows angle dependent NEXAFS spectra

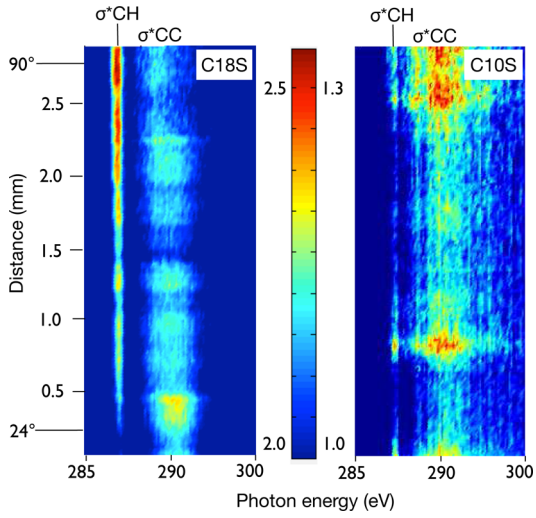

Figure 3. NEXAFS spectra extracted from the curved MOSAIX along the curved axis for the C18S and C10S SAMs. Intensity variations for the σ^* CH and σ^* CC spectral features along the curved axis indicate molecular alignment. The C18S SAMs show significant alignment while the C10S SAMs are not well ordered.

extracted for the different SAM samples. The average tilt angles are also summarized in Figure 4. Since order and orientation are convoluted in NEXAFS the increasing tilt angle observed for SAMs with shorter chain lengths is most likely a sign of lower order and not a more tilted geometry.

In summary, MOSAIX analysis on curved substrates can provide both a rapid overview of the molecular order of large sample sets but also provides all the information required for a detailed, quantitative analysis of molecular tilt angles for samples of interest within the sample set. The acquisition time for the eight samples and five angles included in the curved MOSAIX array was ca. 20 min. This compares with a total acquisition time of approximately 14 h using standard NEXAFS

dx.doi.org/10.1021/co5001162 | ACS Comb. Sci. 2014, 16, 449−453

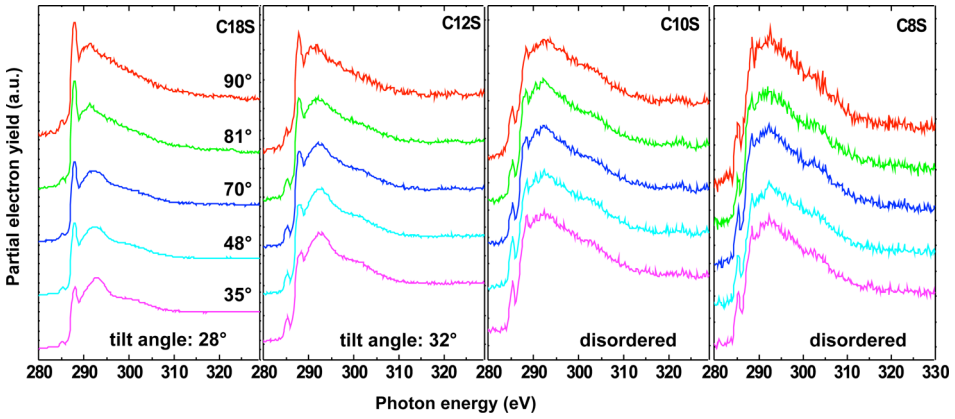

Figure 4. NEXAFS spectra extracted from individual samples in the curved MOSAIX array for the different SAMs. Extracted spectra allow quantitative orientation analysis using methods established for regular NEXAFS spectroscopy.

spectroscopy—a sample throughput increase by a factor of 42. Using MOSAIX analysis on curved surface a typical weeklong beamtime can provide angle runs for approximately 4000 samples, enabling large-scale combinatorial studies using NEXAFS.

EXPERIMENTAL PROCEDURES

Sample Preparation. All samples were prepared on 1 × 1 mm^2 silicon substrates (Microelectronics Inc., San Jose, CA) cleaned by sequential sonication in deionized water, dichloromethylene, acetone, and methanol. In a high vacuum electron beam evaporator (pressure <1 × 10^{-6} Torr), the Si substrates were then coated with a thin adhesion layer of titanium (10 nm) followed by high purity gold (99.99%, 80 nm). Each set of SAMs was assembled by submerging the gold surfaces in 0.1 mM (Sigma-Aldrich) solution of the respective thiols for 16 h. SAMs were fabricated from 1-octanethiol ($C_8H_{18}S$, C8S), 1-decanethiol ($C_{10}H_{22}S$, C10S), 1- dodecanethiol ($C_{12}H_{26}S$, C10S), and octadecanethiol ($C_{18}H_{38}S$, C12S). After assembly, the small samples were placed in a ceramic funnel filter cone and then repeatedly rinsed with 200 proof ethanol (Decon Laboratories, King of Prussia, PA). Once rinsed the individual 1 × 1 mm^2 samples were arranged onto a curved piece of plastic cut out of a falcon tube strip and coated with copper tape. All samples were stored under nitrogen until analysis.

Near-Edge X-ray Absorption Fine Structure (NEXAFS) Microscopy. The NEXAFS images were recorded at the National Institute of Standard and Technology (NIST) U7A beamline at the National Synchrotron Light Source (NSLS) at Brookhaven National Laboratory using the parallel processing imaging endstation described in references 25−27. Briefly, soft X-rays with photon energies near the carbon *K*-edge (270−340 eV; flux ∼5 x10^{10} photons/s (0.1% BW)), was rastered across an 18 × 13 mm^2 area on the sample using an upstream wobbling mirror. A LARIAT system (Large Area Rapid Imaging Analytical Tool, Synchrotron Research Inc.) was used to image the spatially resolved partial electron yield. A microchannel plate electron multiplier detector with a high pass (entrance) voltage grid set at −50 V and a phosphor screen are located in the UHV chamber at 0.5 T pole piece 50 mm away from the sample. Emitted electrons are guided along the magnetic gradient to the detector, amplified, then onto the phosphor screen. Signals from the phosphor translate into partial electron yield (PEY) and a CCD camera located behind the screen captures images. The result is a series of NEXAFS images; the spatial resolution was approximately 50 μm.[25−27] Artifacts from incident beam intensity fluctuations and absorption features in the beamline optics were removed by normalizing the PEY signals by the drain current NEXAFS signal of a clean gold mesh placed upstream of the sample in the path of the X-ray beam.

AUTHOR INFORMATION

Corresponding Authors

*E-mail: dfischer@nist.gov.

*E-mail: weidner@mpip-mainz.mpg.de.

Present Address

[§]J.E.B.: School of Chemical, Biological and Environmental Engineering, Oregon State University, Corvallis, OR, USA

Notes

Certain commercial names are mentioned in this manuscript for purpose of example and do not represent an endorsement by the National Institute of Standards and Technology.

The authors declare no competing financial interest.

ACKNOWLEDGMENTS

The authors thank David G. Castner for support of this work and Lara J. Gamble for collaboration at the synchrotron. T.W. thanks Stephan Imhof and Udo Bertram for photos of the samples. T.W. thanks the Deutsche Forschungsgemeinschaft (DFG, WE4478/2-1) and the EU (Marie Curie Actions Career Integration Grant 322124) for financial support. J.E.B. thanks the National Science Foundation for a research fellowship (NSF Grant 1202620). This work was performed at the NSLS, Brookhaven National Laboratory, which is supported by the U.S. Department of Energy, Division of Materials Science and Division of Chemical Sciences. This work is also a part of the research program of the Max-Planck Society.

REFERENCES

(1) Potyrailo, R.; Rajan, K.; Stoewe, K.; Takeuchi, I.; Chisholm, B.; Lam, H. Combinatorial and high-throughput screening of materials libraries: review of state of the art. *ACS Comb. Sci.* **2011**, *13*, 579−633.

(2) Ulman, A. *Self-Assembled Monolayers of Thiols*, 1 ed.; Academic Press: San Diego, CA, 1998; Vol. *24*.

(3) Acton, O.; Hutchins, D.; Arnadottir, L.; Weidner, T.; Cernetic, N.; Ting, G. G.; Kim, T. W.; Castner, D. G.; Ma, H.; Jen, A. K. Y. Spin-cast and patterned organophosphonate self-assembled monolayer dielectrics on metal-oxide-activated Si. *Adv. Mater.* **2011**, *23*, 1899−1902.

(4) Cernetic, N.; Acton, O.; Weidner, T.; Hutchins, D. O.; Baio, J. E.; Ma, H.; Jen, A. K. Y. Bottom-contact small-molecule n-type organic field effect transistors achieved via simultaneous modification of electrode and dielectric surfaces. *Org. Electron.* **2012**, *13*, 3226−3233.
(5) Hutchins, D. O.; Acton, O.; Weidner, T.; Cernetic, N.; Baio, J. E.; Castner, D. G.; Ma, H.; Jen, A. K. Y. Solid-state densification of spun-cast self-assembled monolayers for use in ultra-thin hybrid dielectrics. *Appl. Surf. Sci.* **2012**, *261*, 908−915.
(6) Hutchins, D. O.; Acton, O.; Weidner, T.; Cernetic, N.; Baio, J. E.; Ting, G.; Castner, D. G.; Ma, H.; Jen, A. K. Y. Spin cast self-assembled monolayer field effect transistors. *Org. Electron.* **2012**, *13* (3), 464−468.
(7) Hutchins, D. O.; Weidner, T.; Baio, J.; Polishak, B.; Acton, O.; Cernetic, N.; Ma, H.; Jen, A. K. Y. Effects of self-assembled monolayer structural order, surface homogeneity and surface energy on pentacene morphology and thin film transistor device performance. *J. Mater. Chem. C* **2013**, *1*, 101.
(8) Wang, Y.; A, A.; Ting, G.; Weidner, T.; Shamberge, P. J.; Ma, H.; Ohuchi, F. S.; Castner, D. G.; K.-Y, J. A. Effect of the phenyl ring orientation in the polystyrene buffer layer on the performance of pentacene thin-film transistors. *Org. Electron.* **2010**, *11*, 1066−1073.
(9) Wang, Y.; Acton, O.; Ting, G.; Weidner, T.; Ma, H.; Castner, D. G.; Jen, A. K. Y. Low-voltage high-performance organic thin film transistors with a thermally annealed polystyrene/hafnium oxide dielectric. *Appl. Phys. Lett.* **2009**, *95*, No. 243302.
(10) Grainger, D. W. DNA nanotechnology: Geometric sorting boards. *Nat. Nanotechnol.* **2009**, *4*, 543−4.
(11) Wu, P.; Castner, D. G.; Grainger, D. W. Diagnostic devices as biomaterials: a review of nucleic acid and protein microarray surface performance issues. *J. Biomater. Sci., Polym. Ed.* **2008**, *19*, 725−753.
(12) Madueno, R.; Raisanen, M. T.; Silien, C.; Buck, M. Functionalizing hydrogen-bonded surface networks with self-assembled monolayers. *Nature* **2008**, *454*, 618−21.
(13) Smits, E. C. P.; Mathijssen, S. G. J.; van Hal, P. A.; Setayesh, S.; Geuns, T. C. T.; Mutsaers, K. A. H. A.; Cantatore, E.; Wondergem, H. J.; Werzer, O.; Resel, R.; Kemerink, M.; Kirchmeyer, S.; Muzafarov, A. M.; Ponomarenko, S. A.; de Boer, B.; Blom, P. W. M.; de Leeuw, D. M. Bottom-up organic integrated circuits. *Nature* **2008**, *455*, 956−959.
(14) Stöhr, J. *NEXAFS Spectroscopy*; Springer-Verlag: Berlin, 1992; Vol. 25.
(15) Outka, D. A.; Stöhr, J.; Rabe, J. P.; Swalen, J. D. The orientation of Langmuir-Blodgett monolayers using NEXAFS. *J. Chem. Phys.* **1988**, *88*, 4076.
(16) Frey, S.; Stadler, V.; Heister, K.; Eck, W.; Zharnikov, M.; Grunze, M.; Zeysing, B.; Terfort, A. Structure of thioaromatic self-assembled monolayers on gold and silver. *Langmuir* **2001**, *17*, 2408−2415.
(17) Heister, K.; Rong, H.-T.; Buck, M.; Zharnikov, M.; Grunze, M.; Johansson, L. S. O. Odd−even effects at the S−metal interface and in the aromatic matrix of biphenyl-substituted alkanethiol self-assembled monolayers. *J. Phys. Chem. B* **2001**, *105*, 6888−6894.
(18) Shaporenko, A.; Mueller, J.; Weidner, T.; Terfort, A.; Zharnikov, M. Balance of structure-building forces in selenium-based self-assembled monolayers. *J. Am. Chem. Soc.* **2007**, *129*, 2232−+.
(19) Leung, B. O.; Hitchcock, A. P.; Brash, J. L.; Scholl, A.; Doran, A.; Henklein, P.; Overhage, J.; Hilpert, K.; Hale, J. D.; Hancock, R. E. W. X-ray spectromicroscopy study of competitive adsorption of protein and peptide onto polystyrene-poly(methyl methacrylate). *Biointerphases* **2008**, *3*, FB27−FB35.
(20) Baio, J. E.; Weidner, T.; Samuel, N. T.; McCrea, K. R.; Baugh, L.; Stayton, P. S.; Castner, D. G. Multi-technique characterization of adsorbed peptide and protein orientation: LK310 and protein G B1. *J. Vac. Sci. Technol. B* **2010**, *28*, C5D1−C5D8.
(21) Baugh, L.; Weidner, T.; Baio, J. E.; Nguyen, P. C. T.; Gamble, L. J.; Slayton, P. S.; Castner, D. G. Probing the orientation of surface-immobilized protein G B1 using ToF-SIMS, sum frequency generation, and NEXAFS spectroscopy. *Langmuir* **2010**, *26*, 16434−16441.
(22) Baio, J. E.; Weidner, T.; Castner, D. G. Characterizing the structure of surface-immobilized proteins: A surface analysis approach. In *Proteins at Interfaces III State of the Art*; American Chemical Society: Washington, DC, 2012; Vol. *1120*, pp 761−779.
(23) Weidner, T.; Dubey, M.; Breen, N. F.; Ash, J.; Baio, J. E.; Jaye, C.; Fischer, D. A.; Drobny, G. P.; Castner, D. G. Direct observation of phenylalanine orientations in statherin bound to hydroxyapatite surfaces. *J. Am. Chem. Soc.* **2012**, *134*, 8750−8753.
(24) Liu, X.; Jang, C.-H.; Zheng, F.; Jürgensen, A.; Denlinger, J. D.; Dickson, K. A.; Raines, R. T.; Abbott, N. L.; Himpsel, F. J. Characterization of protein immobilization at silver surfaces by near edge X-ray absorption fine structure spectroscopy. *Langmuir* **2006**, *22*, 7719−7725.
(25) Fischer, D. A.; Efimenko, K.; Bhat, R. R.; Sambasivan, S.; Genzer, J. Mapping surface chemistry and molecular orientation with combinatorial near-edge X-ray absorption fine structure spectroscopy. *Macromol. Rapid Commun.* **2004**, *25*, 141−149.
(26) Konicek, A. R.; Jaye, C.; Hamilton, M. A.; Sawyer, W. G.; Fischer, D. A.; Carpick, R. W. Near-edge X-ray absorption fine structure imaging of spherical and flat counterfaces of ultrananocrystalline diamond tribological contacts: A correlation of surface chemistry and friction. *Tribol. Lett.* **2011**, *44*, 99−106.
(27) Baio, J. E.; Jaye, C.; Fischer, D. A.; Weidner, T. Multiplexed Orientation and Structure Analysis by Imaging Near-edge X-ray Absorption Fine Structure (MOSAIX) for Combinatorial Surface Science. *Anal. Chem.* **2013**, *85*, 4307−4310.
(28) Laibinis, P. E.; Whitesides, G. M.; Allara, D. L.; Tao, Y. T.; Parikh, A. N.; Nuzzo, R. G. Comparison of the structures and wetting properties of self-assembled monolayers of *n*-alkanethiols on the coinage metal surfaces, copper, silver, and gold. *J. Am. Chem. Soc.* **1991**, *113*, 7152−7167.
(29) Witte, G.; Weiss, K.; Jakob, P.; Braun, J.; Kostov, K. L.; Wöll, C. Damping of molecular motion on a solid substrate: Evidence for electron−hole pair creation. *Phys. Rev. Lett.* **1998**, *80*, 121.
(30) Weidner, T.; Shaporenko, A.; Ballav, N.; Ulman, A.; Zhamikov, M. Modification of alkaneselenolate monolayers by low-energy electrons. *J. Phys. Chem. C* **2008**, *112*, 1191−1198.
(31) Sohn, K. E.; Dimitriou, M. D.; Genzer, J.; Fischer, D. A.; Hawker, C. J.; Kramer, E. J. Determination of the electron escape depth for NEXAFS spectroscopy. *Langmuir* **2009**, *25*, 6341−8.
(32) Dubois, L. H.; Zegarski, B. R.; Nuzzo, R. G. Molecular ordering of organosulfur compounds on Au(111) and Au(100)—Adsorption from solution and in ultrahigh-vacuum. *J. Chem. Phys.* **1993**, *98*, 678−688.
(33) Sambasivan, S.; Hsieh, S.; Fischer, D. A.; Hsu, S. M. Effect of self-assembled monolayer film order on nanofriction. *J. Vac. Sci. Technol. A* **2006**, *24*, 1484.
(34) Schreiber, F. Structure and growth of self-assembling monolayers. *Prog. Surf. Sci.* **2000**, *65*, 151−256.